

# Journal of Materials Chemistry C

Accepted Manuscript



This article can be cited before page numbers have been issued, to do this please use: Z. Wang, Z. Peng, K. Huang, P. Lu and Y. Wang, *J. Mater. Chem. C*, 2019, DOI: 10.1039/C9TC01059A.



This is an Accepted Manuscript, which has been through the Royal Society of Chemistry peer review process and has been accepted for publication.

Accepted Manuscripts are published online shortly after acceptance, before technical editing, formatting and proof reading. Using this free service, authors can make their results available to the community, in citable form, before we publish the edited article. We will replace this Accepted Manuscript with the edited and formatted Advance Article as soon as it is available.

You can find more information about Accepted Manuscripts in the [author guidelines](#).

Please note that technical editing may introduce minor changes to the text and/or graphics, which may alter content. The journal's standard [Terms & Conditions](#) and the ethical guidelines, outlined in our [author and reviewer resource centre](#), still apply. In no event shall the Royal Society of Chemistry be held responsible for any errors or omissions in this Accepted Manuscript or any consequences arising from the use of any information it contains.

## Butterfly-shaped $\pi$ -extended benzothiadiazoles as promising emitting materials for white OLEDs

Zaibin Wang, Zhixing Peng, Kai Huang, Ping Lu\*, Yanguang Wang\*

Received 00th January 20xx,  
Accepted 00th January 20xx

DOI: 10.1039/x0xx00000x

www.rsc.org/

A series of butterfly-shaped D-A-D and D-A-A compounds, composed of benzothiadiazole core and corresponding terminal alkynes were synthesized. Their photophysical properties in different states (solution, film, crystal, and powder) are investigated. Meanwhile, the linear-shaped compounds were prepared accordingly for comparative investigation on their photophysical properties. Three phenomena (aggregation causing quenching, crystal induced emission, aggregation induced emission enhancement) are all observed for the butterfly-shaped compounds. Although the linear-shaped compounds emit brighter light in pristine powders with higher quantum yields, the butterfly-shaped compounds are likely to form crystals and emit colorful light from 473 nm to 622 nm in crystalline state. Moreover, most of them exhibit the mechanochromic character, the color of **2POZ-56** could be reversibly tuned from yellow to red by grinding and fuming. Furthermore, polymorphism-dependent emission was observed for **2POZ-56**, and it could also be used as emissive layer in white organic light emitting diodes.

### Introduction

Fluorescent compounds containing benzothiadiazole (BTD) core have been widely investigated and applied in many disciplines. They are interested as a new class of bioprobes for its absorption in the visible-light region with large molar absorptivity, bright emission with large Stokes shift and high quantum yield, no blinking with good signal-to-noise ratio, high optical and thermal stability in solutions as well as in solids. With these significant characters, the  $\pi$ -extended BTD-derivatives easily break down some limitations normally appeared in the classical scaffolds, such as coumarins, BODIPYs, fluoresceins, rhodamines, cyanines, and phenoxazines, and become star probes for a number of biological analyses in recent years<sup>1</sup>. On the other hand, the electron-deficient BTD core has been extensively used as a key building unit in the construction of donor-acceptor conjugated compounds for optoelectronic applications, such as organic photovoltaics<sup>2</sup>, solar-hydrogen conversion<sup>3</sup>, organic field effect transistor<sup>4</sup>, organic light emitting diode<sup>5</sup> and so on. BTD could also be added between donor and acceptor to enlarge the conjugation and enhance the D-A effect to produce AIEgen with deep red emission for large third-order optical nonlinearity<sup>6</sup> and large reversible mechanochromic behavior for mechano-sensing<sup>7</sup>. When the phenothiazine has two wings of benzothiadiazoles, the resulting A-D-A displays strong

near-infrared (NIR) fluorescence and is fabricated for NIR-OLED<sup>8</sup>. A nearly 800 nm electroluminescent emission could be realized by using naphthothiadiazole instead of benzothiadiazole<sup>9</sup>. In above-mentioned examples of the  $\pi$ -extended BTD derivatives, the conjugation is normally extended through 4,7-positions of the BTD core. In another word, the intramolecular charge transfer (ICT) in the excited state occurs from donor to acceptor through 4,7-positions of BTD core in linear shape. But, change the substituent position as well as the molecular geometry would largely effect on the ICT process as well as their luminescent properties<sup>10</sup>. For instance, experiments show that it is effective to improve the device performance through structural modification. For instance, higher power conversion efficiency could be approached when 5,6-positions of BTD were fluorinated<sup>11</sup>. On this basis, we hereby synthesized a series of conjugated compounds through 5,6-positions of BTD core in butterfly shape. Thus, four different models of the triads with the connection of D-A-D or D-A-A in butterfly or linear shaped were obtained for the systematically investigation of the fluorescent structure-property relationship of the BTD-based conjugated compounds (Scheme 1).

### Results and discussion

#### Synthesis and characterization

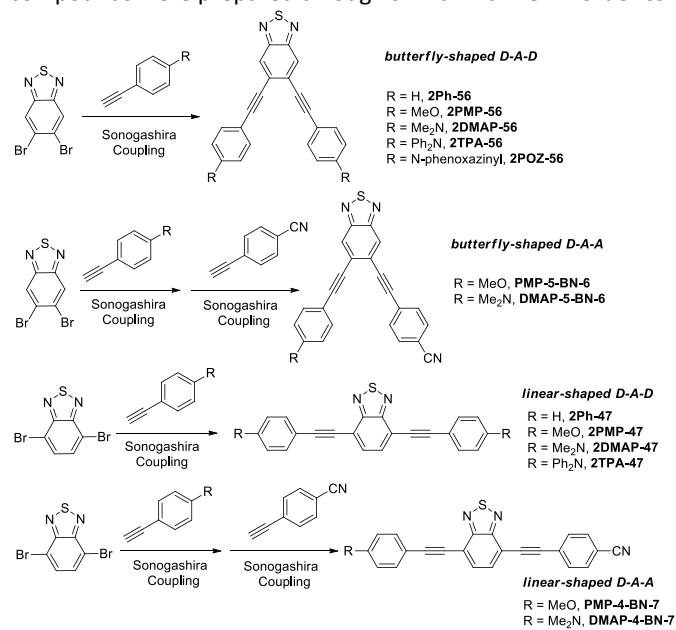
Five butterfly-shaped D-A-D compounds were synthesized in a single step through Sonogashira coupling reactions between 5,6-dibromobenzothiadiazole and corresponding terminal alkynes in moderate to excellent yields. Two butterfly-shaped D-A-A compounds were prepared by firstly coupling of 5,6-dibromobenzothiadiazole with electron-rich alkyne and then

Department of Chemistry, Zhejiang University, Hangzhou 310027, P. R. China.

\*E-mail: pinglu@zju.edu.cn, orgwyg@zju.edu.cn

† Electronic supplementary information (ESI) available: Structural characterization data, TGA, crystallographic data, photophysical spectra, DFT, and CV. CCDC 1887112-1887113 and 1850544-1850549. For ESI and crystallographic data in CIF or other electronic format See DOI: 10.1039/x0xx00000x

the electron-deficient alkyne. Linear-shaped D-A-D and D-A-A compounds were prepared through similar manner in order to



**Scheme 1**  $\pi$ -extended BTD derivatives through 5,6-positions and 4,7-positions

comparative investigation of the fluorescent structure-property relationship of these BTD-containing compounds<sup>12</sup>. Unfortunately, we failed to obtain **2POZ-47** although many efforts had been paid. Among these butterfly-shaped compounds, **2Ph-56** has been previously reported as an intermediate in the preparation of quinoxalenediynes<sup>13</sup>. Others were firstly synthesized and fully characterized by <sup>1</sup>H and <sup>13</sup>C NMR (Figures S1-S22), IR, HRMS and further confirmed by their single crystal analysis. The crystallographic data are summarized in Table S1. Compounds in butterfly-shaped are thermally stable on the basis of TGA analysis (Figure S23, Table1). The decomposition temperature, obtained at 5% weight loss, is 291 °C for **2Ph-56**. Substitution on **2Ph-56** with methoxy, dimethylamino, and diphenylamino groups significantly increase the thermal stability. With phenoxazine substituted, decomposition temperature of **2POZ-56** is determined to be 436 °C. In comparison to these butterfly-shaped compounds, the linear-shaped compounds presented higher decomposition temperatures, accordingly (Figure S24).

### Absorption and emission of these compounds in solutions

The synthesized compounds are soluble in normal organic solvents, such as cyclohexane (CH), toluene (Tol), dioxane (DIO), tetrahydrofuran (THF), and dichloromethane (DCM). Absorption spectra were recorded in a concentration of  $2 \times 10^{-5}$  mol L<sup>-1</sup> in tetrahydrofuran (Figure 1, Table 1). **2Ph-56** absorbs light at two bands with the maximum absorption wavelength of 373 nm and the molar absorptivity of  $1.87 \times 10^4$  L mol<sup>-1</sup> cm<sup>-1</sup>. It emits light at 424 nm with a Stokes shift of 51 nm and a quantum yield of 19%. By tethering two methoxy at both ends, **2PMP-56** presents red-shifted absorption as well as red-shifted emission with higher molar absorptivity and higher quantum yield as we expected. Moreover, a larger Stokes shift (85 nm) is observed for **2PMP-56** in comparison with that of **2Ph-56**. Replacement of methoxy with dimethylamino, absorption and emission spectra of **2DMAP-56** are further bathochromically shifted. Thus, **2DMAP-56** absorbs light at 439 nm with molar absorptivity of  $2.58 \times 10^4$  L mol<sup>-1</sup> cm<sup>-1</sup> and emits light at 600 nm with quantum yield of 13%. The large Stokes shift (161 nm) indicates the excellent electronic communication between donor and acceptor which directly results in the decreased quantum yield when two compounds with similar molar absorptivities are compared<sup>14</sup>. With diphenylamino substituted (**2TPA-56**), the electron donating ability from nitrogen to BTD core is partially inhibited because of the propeller structure of triphenylamine. Therefore, larger molar absorptivity ( $2.76 \times 10^4$  L mol<sup>-1</sup> cm<sup>-1</sup>) and smaller Stokes shift are recorded (140 nm) for the dilute THF solution of **2TPA-56**. It shows the largest quantum yield (35%) among these butterfly-shaped D-A-D as well as D-A-A compounds. With phenoxazinyl substituted, **2POZ-56** absorbs light at 325 nm with the molar absorptivity of  $1.84 \times 10^4$  L mol<sup>-1</sup> cm<sup>-1</sup>, but without fluorescence.

To linear-shaped D-A-D compounds, absorption and emission spectra are all red-shifted with higher molar absorptivities and higher quantum yields in comparison with those of the corresponding butterfly-shaped D-A-D compounds. The highest quantum yield (95%) is obtained for **2PMP-47**, while the largest maximum emission wavelength (607nm) is recorded for **2DMAP-47**.

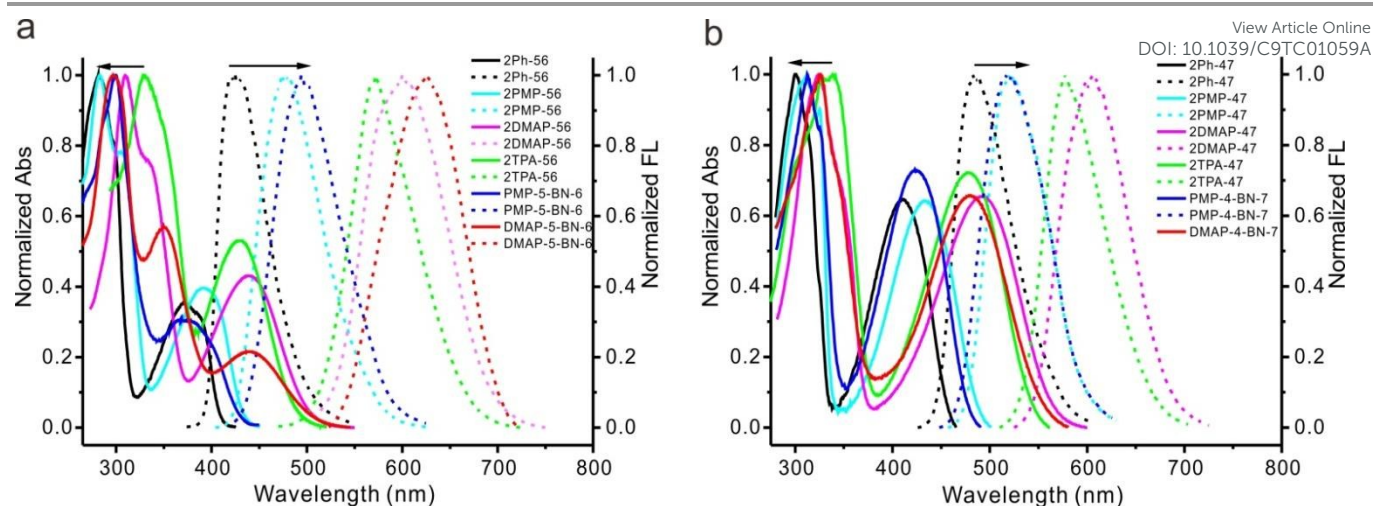


**Figure 1** (a) Absorptions and emissions of butterfly-shaped compounds in THF; (b) Absorptions and emissions of linear-shaped compounds in THF.

**Table 1** Photophysical properties of these compounds in different states as well as their thermal stability

Compounds	$\lambda_{\max}^{\text{abs}}$ ( $\epsilon \times 10^4/\text{L mol}^{-1} \text{ cm}^{-1}$ ) <sup>[a]</sup>	$\lambda_{\max}^{\text{em}}$ [a, b]	Stokes	$\lambda_{\max}^{\text{em}}$ powder <sup>[c]</sup>	$\lambda_{\max}^{\text{em}}$ crystal	$\lambda_{\max}^{\text{em}}$ film <sup>[d]</sup>	$\Phi$ (%) <sub>THF</sub> <sup>[e]</sup>	$\Phi$ (%) <sub>film</sub> <sup>[e]</sup>	$T_d$ (°C) <sup>[f]</sup>
<b>2Ph-56</b>	281(5.20) 373(1.87)	424 (386)	51	484	-----	-----	19	2.2	291
<b>2PMP-56</b>	283(6.20) 393(2.47)	478 (398)	85	498	473	468	31	1.8	395
<b>2DMAP-56</b>	309(5.93) 439(2.58)	600 (498)	161	577	592	550	13	1.5	385
<b>2TPA-56</b>	329(5.17) 432(2.76)	572 (433)	140	550	557	-----	35	7.1	410
<b>2POZ-56</b>	287(5.13) 325(1.84)	-----	-----	563	573 <sup>g</sup> 627 <sup>h</sup>	-----	0	2.9	436
<b>2Ph-47</b>	300(4.03) 411(2.64)	483(416)	72	478	-----	469	88	20	524
<b>2PMP-47</b>	312(4.35) 433(2.82)	519 (449)	86	562	-----	530	95	24.4	457
<b>2DMAP-47</b>	324(5.38) 492(3.52)	607 (510)	115	630	-----	-----	38	13.4	389
<b>2TPA-47</b>	339(5.5) 478(4.0)	577 (492)	99	630	-----	576	70	25.2	508
<b>PMP-5-BN-6</b>	300(6.05) 368(1.83)	494 (380)	126	511	492	-----	22	1.2	418
<b>DMAP-5-BN-6</b>	298(5.75) 350(3.28) 442(1.25)	626 (352)	184	585	601	-----	2	3.7	389
<b>PMP-4-BN-7</b>	313(4.38) 423(3.22)	517 (436)	94	526	-----	533	92	14.6	466
<b>DMAP-4-BN-7</b>	325(3.93) 480(2.60)	-----	-----	637	-----	-----	0	11.8	436

[a] Measured in THF solution,  $c=2 \times 10^{-5}$  M; [b] excitation wavelength indicated in parenthesis; [c] pristine powder; [d] Films are prepared by spin-coating of dilute chlorobenzene solution on quartz plate; [e] Quantum yields are obtained from integrating sphere; [f] Decomposition temperature is determined by TGA when the weight loss is 5%; [g] emission from crystal I; [h] emission from crystal II

To butterfly-shaped D-A-A compounds, **PMP-5-BN-6** absorbs light at two bands (300 nm and 368 nm) and emits light at 494 nm with Stokes shift of 126 nm and quantum yield of 22%.

**DMAP-5-BN-6** absorbs light at three bands (298 nm, 350 nm, and 442 nm) and emits light at 626 nm with the largest Stokes shift of 184 nm and relative low quantum yield of 2%. A better conjugation is seen in the case of the linear-shaped D-A-A. Thus, absorption and emission spectra of **PMP-4-BN-7** are all red-shifted with Stokes shift of 94 nm and quantum yield of 92%. **DMAP-4-BN-7** absorbs light at 325 nm and 480 nm, but without fluorescence.

Based on these findings, some preliminary conclusions could be made. The maximum absorption and emission wavelengths largely depend on the type of the substituents and the resultant electronic communication between the donor and acceptor. Among these donors, dimethylamino is the most powerful electron donor followed by diphenylamino and methoxy. Substitution on 4,7-positions of BTD provides better conjugation and higher quantum yields in comparison with substitution on 5,6-positions of BTD.

#### Solvent effect on absorption and emission of these compounds

It is common that polar molecule shows the solvatochromic effect and the extent depends on the dipole moment change of the molecule in excited state and ground state. In general speaking, the larger the dipole moment changes, the bigger the solvatochromic effect is<sup>15</sup>. To these butterfly-shaped and linear-shaped compounds, we record their absorption and emission in various solvents (Figure 2, Figures S25-S26) and the corresponding data are summarized in Table S2. Absorption spectra of **2Ph-56** in various solvents are almost identical, but with red-shifted emission from 400 nm, 412 nm, 412 nm, 424 nm, to 430 nm as the solvent changes from CH, Tol, DIO, THF, to DCM. When

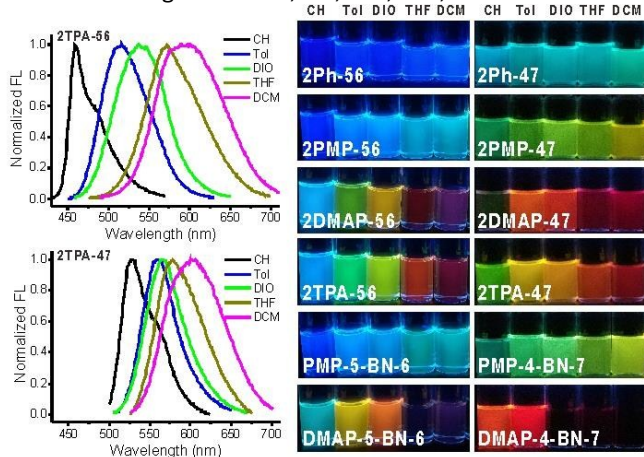


**Figure 2** Solvatochromism of 2TPA-56 (up left) and 2TPA-47 (down left); solutions of butterfly-shaped (middle) and linear-shaped compounds (right) under UV lamp

methoxy substituted on both ends, absorption spectra of **2PMP-56** keep the same, while their emission spectra change a lot. The maximum emission wavelength ranges from 416 nm to 488 nm as the solvent changes from CH to DCM. With dimethylamino substituted, the maximum emission

wavelength of **2DMAP-56** changed from 463 nm, 531 nm, 561 nm, 600 nm, to 602 nm as the solvent changes from CH, Tol, DIO, THF, to DCM, while the solution color under UV lamp changes from blue, green, yellow, red, to purple, accordingly. Similar solvatochromic effect is observed for **2TPA-56** (Figure 2, up left). **2POZ-56** is fluorescent in cyclohexane, toluene, and dioxane. The maximum emission wavelength is 481 nm, 569 nm, and 595 nm, accordingly. However, it is non-fluorescent in tetrahydrofuran and dichloromethane.

When linear-shaped D-A-D compounds are tested, solvatochromic effect still exists but with less influenced in comparison with those corresponding butterfly-shaped D-A-D compounds. In contrast to **2TPA-56**, **2TPA-47** presents smaller solvatochromic effect (Figure 2, down left). The largest solvatochromic effect is observed for the butterfly-shaped **DMAP-5-BN-6**, which emits light at 480 nm in cyclohexane and 626 nm in tetrahydrofuran, respectively. When the molecule is excited, electron transition occurs from  $S_0$  to  $S_1$ . Both energy levels of  $S_0$  and  $S_1$  would be decreased as the molecule surround by solvents because of the solvation. The decreased degree depends on the dipole moments of  $S_0$  and  $S_1$  as well as the solvent polarity. Generally speaking, the dipole moment of  $S_1$  is larger than that of  $S_0$  that directly results in the Stokes shift in non-polar solvent. As the D-A compound is tested, not only locally excited (LE) emission could be observed but the intramolecular charge transfer (ICT) emission also. In these cases, the polar solvent is more likely to solvate the excited state of the ICT which further reduces the energy gap and results in the red-shifted emission. In comparison with linear-shaped D-A-D compounds, the butterfly-shaped D-A-D compounds obviously possess larger dipole moments in ground states because of the molecular geometry. Theoretical calculation confirmed this order (Table S3). To the series of **2Ph-56**, **2PMP-56**, **2DMAP-56**, and **2TPA-56**, the dipole moments of these compounds in ground states are calculated to be 5.0, 5.6, 12.2, and 8.1 D, respectively. By applying the modified Lippert-Mataga equation<sup>16</sup>, the dipole moment changes for these compounds are found to be 10.1, 16.5, 18.3, and 22.4 D, respectively. The bigger the dipole moment change, the more red-shifted of emission. To the linear-shaped D-A-D compounds of **2Ph-47**, **2PMP-47**, **2DMAP-47**, and **2TPA-47**, the dipole moment changes are obtained in smaller values (8.3, 11.0, 10.4, and 12.6 D, respectively) in comparison with those of the butterfly-shaped compounds. Therefore, the linear-shaped D-A-D compounds present smaller solvatochromism, accordingly. To D-A-A compounds, the linear-shaped compounds presented larger dipole moment in the ground state than the one in butterfly-shaped because of longer efficient conjugation length<sup>17</sup> from the donor to acceptor. Thus, to the pair of **PMP-5-BN-6** and **PMP-4-BN-7**, although **PMP-4-BN-7** has larger dipole moment in ground state, **PMP-5-BN-6** presents larger dipole moment change based on the modified Lippert-Mataga equation (Table S3). Thus, as the solvent changes from cyclohexane to dichloromethane, the emission of **PMP-5-BN-6** shifts from 422 nm to 500 nm in DCM, while **PMP-4-BN-7** shifts from 475 nm to 525 nm in DCM accordingly. Above all, the larger

solvatochromism is observed for those compounds in butterfly-shaped because these compounds possess larger dipole moment changes.

#### Emissions of these compounds in nanoparticles or tiny crystals in aqueous THF solutions

These compounds are easily to form nanoparticles or tiny crystals as we quickly pour water into their dilute THF solutions. **2Ph-56** presents a gradually red-shifted emission with a gradually decreased quantum yield as water fraction increases. When the water fraction increased to 95%, TEM shows the formation of nanoparticle with the diameter about 100 nm which was further confirmed by DLS (Figure 3, left column). Thus, a typical aggregation causing quenching (ACQ) occurs in this case. With methoxy substituted, **2PMP-56** shows the red-shifted emission along with the decreased quantum yield as water fraction reaches 70%. As water fraction increased to 80% and beyond, precipitation occurs with the

emission turns off. The precipitation could even be seen by the naked eyes, probably due to the limited solubility. Increment of water fraction to 95%, both TEM and DLS indicate the formation of nanoparticles with the diameter about 100 nm (Figure S27). At this point, the fluorescence is completely turned off. As a comparison, **PMP-5-BN-6** presents almost identical phenomenon (Figure 3, right; Figure S28). On the contrary, with the dimethylamino substituted, emission of **2DMAP-56** in THF solution is turned off as the water fraction ranges from 20% to 60% (Figure S29). The emission comes back when the water fraction reaches 70% but with significantly blue-shifted. A much broad emissive peak is recorded as the water fraction reaches 95%. In this case, nanoparticles are formed that are confirmed by TEM and DLS. When the unsymmetrical D-A-A is tested, a relatively broad and weak emission from **DMAP-5-BN-6** is quenched as the water

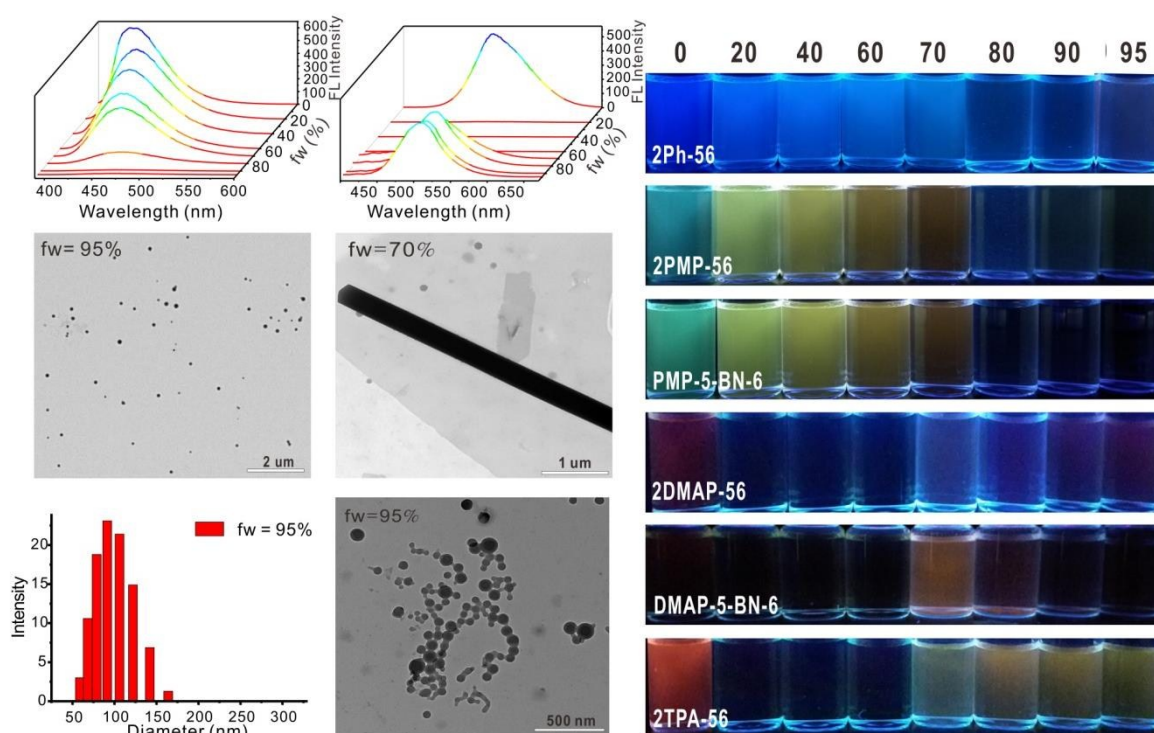


**Figure 3** Emissions and shapes of **2Ph-56** (left column) and **2TPA-56** (middle column), as well as aqueous THF solutions of these butterfly-shaped compounds under UV lamp (right column)

fraction ranges from 20% to 60% (Figure S30). When the water fraction reaches 70%, tiny crystal forms and emits bright light at 566 nm. The bright tiny crystals could be seen by naked eyes and confirmed by TEM. In this case, it is a typical crystalline induced emission (CIE). Beyond 70%, **DMAP-5-BN-6** forms nanoparticles with the aggregation caused quenching emission (ACQ). To compound **2TPA-56**, emission at 572 nm in pure THF solution is gradually quenched as water fraction ranges from 20% to 60% (Figure 3, middle column). As water fraction reaches 70%, tiny crystals form and emit light at 567 nm. When the water fraction reaches 80% and beyond, nanoparticles form and emit light at 563 nm, indicating the aggregation induced emission enhancement (AIEE). After all,

three normal phenomena (ACQ, CIE, and AIEE) are all observed relying on the different substituted groups and different fraction of water.

#### Emission of these compounds in solid states

We then move onto the investigation of the emissions of these compounds in solid states which is important because the practical usage of these compounds in optoelectronic devices is mostly in solid state. Solid states are classified into four categories, including crystalline, pristine powder, ground powder and pure film.

Six single crystals for six butterfly-shaped compounds are obtained by slowly evaporation of the appropriate solvents

except for the **2Ph-56**. Single crystal of **2PMP-56** is transparency and emits light at 473 nm which is slightly blue-shifted in comparison with its emission in dilute THF solution (478 nm) (Figures 4 and S31 a&b, Table 1). With dimethylamino substituted, single crystal of **2DMAP-56** is bright red under UV lamp. Similar to the observations in solution, crystal emission of **2TPA-56** is blue-shifted in comparison with the crystal emission of **2DMAP-56** because of the propeller structure of triphenylamine and the decreased conjugation. With cynao substituted, the crystal emission of **PMP-5-BN-6** is bright green, while the crystal emission of **DMAP-5-BN-6** is orange red. Polymorphism-dependent emission (PDE) was observed for **2POZ-56**. By slowly evaporating the dilute solution of **2POZ-56** in DCM/MeOH/Acetone/n-Hexane, two different crystals (I and II) were separated and picked up by tweezers (Figures 5 and

S31b). Crystal I emits light at 573 nm, while crystal II emits light at 627 nm because of the different molecular stacking modes. To the emissions of these compounds in pristine powders (Figures 4, S31c and S32a, Table 1), it could be clearly seen from photos that the linear-shaped compounds, no matter it is symmetrical or unsymmetrical, are all brighter than the corresponding compounds in butterfly-shaped under UV lamp. Undoubtedly, the linear-shaped compounds present higher quantum yields in pristine powders. Moreover, most of the linear-shaped compounds provide red-shifted emissions in comparison with those corresponding compounds in butterfly-shaped except for the pair of the unsubstituted **2Ph-56** and **2Ph-47**. The biggest change could be seen for the pair of **2TPA-56** and **2TPA-47**. **2TPA-56** emits light at 550 nm in pristine powder, while **2TPA-47** emits light at 630 nm. It might be the

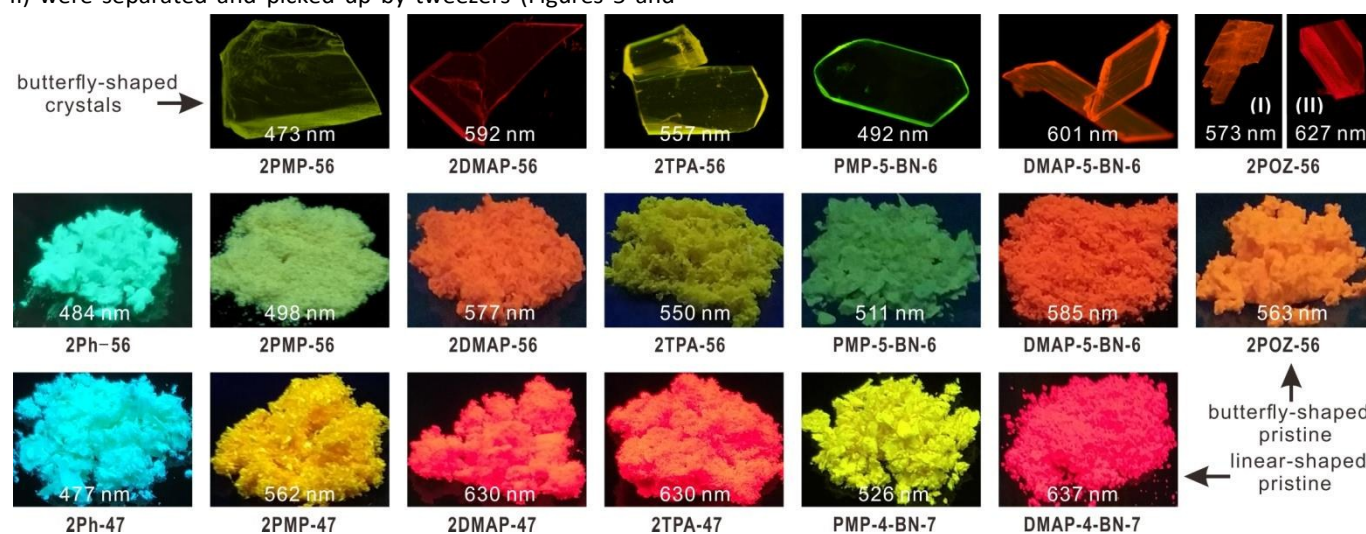


**Figure 4** Photos of these compounds under UV lamp, butterfly-shaped compounds in crystalline (above), butterfly-shaped compounds in pristine (middle), linear-shaped compounds in pristine (down)

steric hindrance existing in **2TPA-56** which inhibits the effective conjugation between TPA and BTB in a certain degree.

Some of them are fabricated in films by spin coating the dilute chlorobenzene solutions on quartz plates (Figures S31d and S32b) and the fluorescent results are summarized in Table 1. To these films, blue-shifted emissions are observed in comparison with those compounds in pristine powders except the linear-shaped unsymmetrical **PMP-4-BN-7**.

#### Mechanochromic characters of these compounds

Some compounds show mechanochromic characters. By grinding the pristine powder of **2Ph-56**, the emission spectra kept same. Both of the two states (in pristine and in ground) emit light at 484 nm (Figure S33). In comparison with this, linear-shaped **2Ph-47** presents mechanochromic property. By grinding the pristine powder of **2Ph-47**, the maximum emission wavelength changes from 478 nm to 504 nm (Figure S34). By fuming the sample with DCM and grinding the sample, the maximum emission wavelength changes into 534 nm. Fuming the ground sample with DCM again, the emission spectrum keeps the same and could not be tuned back. In

another word, the mechanofluorochromic effect is not reversible for **2Ph-47**. XRD tells us that the molecular stacking mode in pristine, fir-grinding, and sec-grinding are not the same.

With methoxy substituted, **2PMP-56**, **2PMP-47**, **PMP-5-BN-6** and **PMP-4-BN-7** show slightly change in emission spectra before and after grinding (Figure S35). With dimethylamino

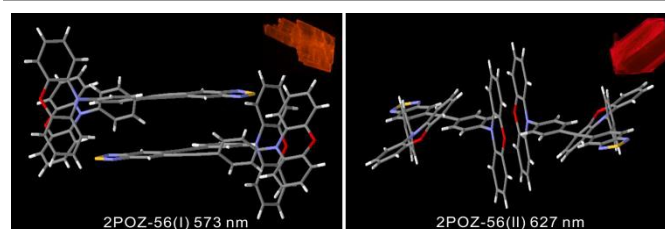


**Figure 5** Crystals (I and II) of **2POZ-56** and their molecular stacking modes

substituted, **2DMAP-56** shows the reversible emissive spectra from 607 nm to 581 nm by grinding and fuming. The color change could be clearly seen by putting the sample under UV lamp (Figure S36). Similar alternation is observed for **2DMAP-**

47, but with smaller difference (10 nm) in maximum emission wavelengths (Figure S37). To the butterfly-shaped **DMAP-5-BN-6** (Figure S38) and linear-shaped **DMAP-4-BN-7** (Figure S39), reversible emissive spectra are also recorded. Both of them show 15 nm differences in maximum emission wavelength by grinding and fuming. Grinding **2TPA-56** brings a slightly red-shifted emission from 550 nm to 556 nm, while grinding **2TPA-47** brings a slightly blue-shifted emission from 630 nm to 626 nm (Figure S40). The biggest and reversible change is seen for **2POZ-56**. By grinding the pristine powder of **2POZ-56**, the maximum emission wavelength changes from 563 nm to 621 nm. Fuming the ground powder with DCM for 2 minutes, the emission wavelength turns back to 569 nm and the color changes accordingly from red to yellow under UV lamp (Figure 6).

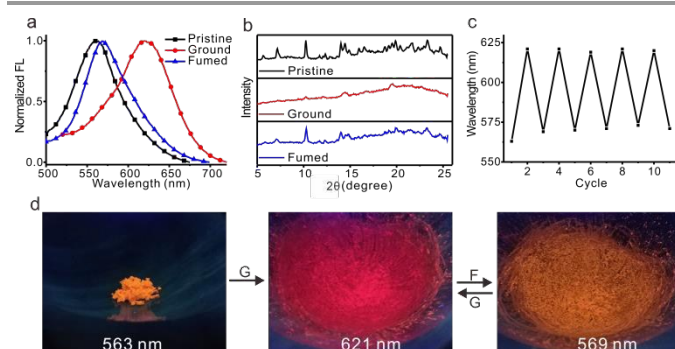


**Figure 6** Emission spectra (a) and XRD diffractions (b) of **2POZ-56** before and after grinding/fuming; (c) Reversible changes of emission intensities of **2POZ-56** by grinding and fuming; (d) Photos under UV lamp

### Electrochemical properties of the butterfly-shaped compounds

Cyclic voltammetric studies are carried out in solutions (MeCN:DCM = 3:1) in order to obtain the oxidation and reduction potentials and to estimate the frontier orbital levels (HOMO and LUMO) of the butterfly-shaped compounds. Results are summarized in Figure S41 Table S4. The energy gaps obtained from the electrochemical studies are in good accordance with the energy gaps obtained from theoretical calculation as well as from UV measurements in dilute THF solutions except for an incomprehensible drop of energy gap for **2POZ-56** from CV measurement. Compounds substituted with dimethylamino group (**2DMAP-56** and **DMAP-5-BN-6**) or phenoxazinyl group (**2POZ-56**) present smaller energy gaps with longer emission wavelengths.

### Electroluminescent properties

Several butterfly-shaped compounds were further applied to estimate their utilities for OLEDs. Thus, three devices with a sandwiched structure of ITO / PEDOT : PSS (40 nm) /  $m_{\text{Compd}}$  :  $m_{\text{PVK}}$  (1 : 16) / TPBI (30nm) / LiF (1 nm) / Al (60 nm) were designed and fabricated by respectively using **DMAP-5-BN-6**, **2TPA-56**, and **2POZ-56** (Figures S42, S43 and 7). Results are summarized in Table S5. A white OLED device was achieved by doping 2POZ-56 in PVK. The device emits light at a broad range with two peaks of 403 nm and 555 nm (CIE = 0.32, 0.35) at a voltage of 7v. At a brightness of 100 cd m<sup>-2</sup>, the external quantum yield (0.29%), the luminous efficiency (0.53 cd A<sup>-1</sup>),

and the power efficiency (0.27 lm W<sup>-1</sup>) were obtained. The origin of the blue band emission could be ascribed to PVK emission on the basis of the controlled experiment.

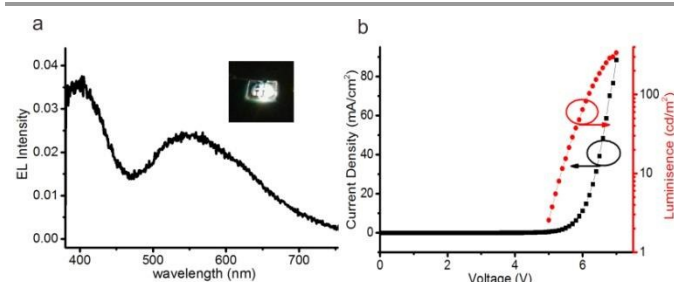


**Figure 7** EL a) Spectrum of **2POZ-56** based device operating at a voltage of 7 v. Inset: Image of device; b) Current-density-voltage (L-J-V) characteristics

### Conclusions

In this work, we designed and synthesized a series of butterfly-shaped D-A-D and D-A-A compounds by using benzothiadiazole core as electron acceptor. Meanwhile, the linear-shaped compounds were prepared accordingly for comparative investigation on their photophysical properties in different states. Although the linear-shaped compounds present higher molar absorptivities and higher solution quantum yields because of the better conjugation, larger solvatofluorochromic effects are observed for the butterfly-shaped compounds. By pouring water into THF solutions, three phenomena (aggregation causing quenching, crystal induced emission, aggregation induced emission enhancement) are all observed for the butterfly-shaped compounds and the variation largely depends on the substituted group and the water fraction. Although the linear-shaped compounds emit bright light in pristine powders with higher quantum yields, the butterfly-shaped compounds are likely to form crystals and emit colorful light from 473 nm to 622 nm in crystalline state. Furthermore, polymorphism-dependent emission was observed for **2POZ-56**. It is also noticeable that most of them exhibit the mechanochromic character. By grinding and fuming, the color of **2POZ-56** could be reversibly tuned from red to yellow. Finally, **2POZ-56** could be used in the fabrication of white OLED device.

### Conflicts of interest

There are no conflicts to declare.

### Acknowledgements

The authors thank Prof. Yizheng Jin for providing help in the fabrication of OLED devices and thank the National Natural Science Foundation of China (21871229).

### Notes and references

- (a) B. A. D. Neto, P. H. P. R. Carvalho and J. R. Correa, *Acc. Chem. Res.*, 2015, **48**, 1560-1569; (b) B. A. D. Neto, P. H. P. R.

- Carvalho, D. C. B. D. Santos, C. C. Gatto, L. M. Ramos, N. M. de Vasconcelos, J. R. Corrêa, M. B. Costa, H. C. B. de Oliveira and R. G. Silva, *RSC Adv.*, 2012, **2**, 1524–1532.
- 2 (a) J. Du, M. C. Biewer and M. C. Stefan, *J. Mater. Chem. A*, 2016, **4**, 15771–15787; (b) S. Zeng, L. Yin, C. Ji, X. Jiang, K. Li, Y. Li and Y. Wang, *Chem. Commun.*, 2012, **48**, 10627–10629; (c) X. Liu, R. Zhu, Y. Zhang, B. Liu and S. Ramakrishna, *Chem. Commun.*, 2008, 3789–3791; (d) J. Lu, F. Liang, N. Drolet, J. Ding, Y. Tao and R. Movileanu, *Chem. Commun.*, 2008, 5315–5317; (e) M. Helgesen, S. A. Gevorgyan, F. C. Krebs and R. A. J. Janssen, *Chem. Mater.*, 2009, **21**, 4669–4675
- 3 J. Chen, C.-L. Dong, D. Zhao, Y.-C. Huang, X. Wang, L. Samad, L. Dang, M. Shearer, S. Shen and L. Guo, *Adv. Mater.*, 2017, **29**, 1606198
- 4 (a) M. Zhang, H. N. Tsao, W. Pisula, C. Yang, A. K. Mishra and K. Mullen, *J. Am. Chem. Soc.* 2007, **129**, 3472–3473; (b) X. Zhang, H. Bronstein, A. J. Kronemeijer, J. Smith, Y. Kim, R. J. Kline, L. J. Richter, T. D. Anthopoulos, H. Sirringhaus, K. Song, M. Heeney, W. Zhang, I. McCulloch, D. M. DeLongchamp, *Nat. Commun.* 2013, **4**, 2238.
- 5 (a) F. Ni, Z. Wu, Z. Zhu, T. Chen, K. Wu, C. Zhong, K. An, D. Wei, D. Ma and C. Yang, *J. Mater. Chem. C*, 2017, **5**, 1363–1368; (b) J. Liu, L. Bu, J. Dong, Q. Zhou, Y. Geng, D. Ma, L. Wang, X. Jing and F. Wang, *J. Mater. Chem.*, 2007, **17**, 2832–2838; (c) Y. Zhang, Z. Chen, X. Wang, J. He, J. Wu, H. Liu, J. Song, J. Qu, W. T.-K. Chan and W.-Y. Wong, *Inorg. Chem.*, 2018, **57**, 14208–14217; (d) Y. Zhang, Z. Chen, J. Song, J. He, X. Wang, J. Wu, S. Chen, J. Qu and W.-Y. Wong, DOI: 10.1039/C8TC05383A
- 6 S. Chen, Z. Qin, T. Liu, X. Wu, Y. Li, H. Liu, Y. Song and Y. Li, *Phys.Chem. Chem. Phys.*, 2013, **15**, 12660–12666.
- 7 T. Jadhav, B. Dhokale and R. Misra, *J. Mater. Chem. C*, 2015, **3**, 9063–9068.
- 8 (a) L. Yao, S. Zhang, R. Wang, W. Li, F. Shen, B. Yang and Y. Ma, *Angew. Chem. Int. Ed.*, 2014, **53**, 2119–2123; (b) S. Xue, Y. Wu, Y. Lu, X. Xu, Q. Sun and W. Yang, *J. Mater. Chem. C*, 2017, **5**, 11700–11707. View Article Online  
DOI: 10.1039/C9TC01059A
- 9 T. Liu, G. Xie, C. Zhong, S. Gong and C. Yang, *Adv. Funct. Mater.* 2018, **28**, 1706088
- 10 (a) B. Sk, S. Khodia and A. Patra, *Chem. Commun.*, 2018, **54**, 1786–1789.
- 11 (a) Z. Li, J. Lu, S.-C. Tse, J. Zhou, X. Du, Y. Tao and J. Ding, *J. Mater. Chem.*, 2011, **21**, 3226–3233; (b) J. Zhang, W. Chen, A. J. Rojas, E. V. Jucov, T. V. Timofeeva, T. C. Parker, S. Barlow and S. R. Marder, *J. Am. Chem. Soc.*, 2013, **135**, 16376–16379; (c) J. W. Jung, F. Liu, T. P. Russell and W. H. Jo, *Adv. Mater.*, 2015, **27**, 7462–7468; (d) L. Cartwright, A. Iraqi, Y. Zhang, T. Wang and D. G. Lidzey, *RSC Adv.*, 2015, **5**, 46386–46394; (e) J.-L. Wang, F. Xiao, J. Yan, Z. Wu, K.-K. Liu, Z.-F. Chang, R.-B. Zhang, H. Chen, H.-B. Wu and Y. Cao, *Adv. Funct. Mater.*, 2016, **26**, 1803–1812
- 12 (a) B. A. D. Neto, A. S. Lopes, G. Ebeling, R. S. Goncalves, V. E. U. Costa, F. H. Quina and J. Dupont, *Tetrahedron*, 2005, **61**, 10975–10982; (b) P. Gautam, R. Maragani and R. Misra, *RSC Adv.*, 2015, **5**, 18288–18294
- 13 S. A. Valenzuela, A. J. Cortes, Z. J. E. Tippins, M. H. Daly, T. I. E. Keel, B. F. Gherman and J. D. Spence, *J. Org. Chem.*, 2017, **82**, 13297–13312
- 14 Z. Peng, Z. Wang, Z. Huang, S. Liu, P. Lu and Y. Wang, *J. Mater. Chem. C*, 2018, **6**, 7864–7873
- 15 (a) J. G. Speight in *Lange's Handbook Of Chemistry*, section two, Laramie, Wyoming, 2004, 899–923. (b) Z. R. Grabowski, K. Rotkiewicz and W. Rettig, *Chem. Rev.*, 2003, **103**, 3899. (c) S. P. Wang, X. J. Yan, Z. Cheng, H. Y. Zhang, Y. Liu and Y. Wang, *Angew. Chem. Int. Ed.*, 2015, **54**, 13068–13072.
- 16 (a) Joseph R, *Principles of Fluorescence Spectroscopy*, 2<sup>nd</sup> edition, 1999. (b) J. Feng, X. Chen, Q. Han, H. Wang, P. Lu, Y. Wang, *Journal of Luminescence*, 2011, **131**, 2775–2783
- 17 Z. Zhao, X. Xu, F. Wang, G. Yu, P. Lu, Y. Liu, D. Zhu, *Synthetic Metals*, 2006, **156**, 209–214

